VOLUMETRIC SOLAR ABSORBER AND PERFORMANCE CHARACTERISTICS

*Bekir Sami Yilbas
Professor, ME Department, KFUPM
Dhahran, Saudi Arabia

Osman K. Siddiqui
Ph.D. Candidate, ME Department, KFUPM
Dhahran, Saudi Arabia

ABSTRACT

Volumetric solar absorption system accommodating the absorber plate in a rectangular channel is investigated. The influence of the location of the absorbing plate on the heat transfer and hydrodynamic characteristics are examined in the channel. Phase change material (Lauric acid) of 5% concentration is used to increase the thermal storage capacity of the working fluid and water is incorporated as the carrier fluid in the channel. Thermal performance and pump power loss parameters are introduced to assess the thermal performance of the volumetric solar absorption system. The findings revealed that thermal performance parameter attains the highest value for the absorber plate location at the center and bottom of the channel. The pump power loss parameter becomes the highest for the absorber plate location at the mid-height of the channel.

INTRODUCTION

Solar energy harvesting is one of the current research fields, which takes the attention of researchers for industrial and domestic energy utilization. Improved solar absorption is one of the thermal preferences because of the minimal environmental impact. On the other hand, efficiency of such systems is limited due to the low thermal performance of the working fluid in the absorbing system; in which vase, the low thermal storage capacity of the working fluid has an adverse effect on the system performance. Introducing the phase change particles (P.C.M) in the thermal system enhances the thermal storage capacity of the working fluid through utilizing the latent heat of PCM. The solar absorption can also be improved via introducing the selective surfaces in the systems. However, radiation losses at high temperatures from the selective surface lower the amount of energy harvested from the Sun. Therefore, the location of solar absorber plate in the thermal system becomes critical for the efficient harvesting process.

Veeraragevan et al. [1] studied the volumetric absorption of the solar radiation and introduced the analytical solution for temperature increase in the carrier fluid. They presented optimum total system efficiency in terms of receiver length and provided convenient tools for predicting the system performance. Heat transfer analysis in relation to micro-encapsulated PCM slurry flow in circular ducts was investigated by Charunyakorn et al. [2]. They demonstrated that use of slurry flow enhanced the heat transfer rates to the working fluid by 2-3 folds as compared to that of the single phase flow. Roy and Sengupta [3] studied the thermal performance of micro-encapsulated phase change particles. They showed that thick walled micro-capsules were unable to withstand thermal cycling at elevated temperatures. Thermal performance of slurry consisting of phase change material and the carrier fluid were studied by Choi et al. [4]. They introduced three regions of importance to identify the melting in the flow systems. Thermal analysis for slurry flow in a circular tube was carried out by Goel et al. [5]. They indicated that tube wall temperature could be increased slightly above the melting temperature of phase change particles to achieve high thermal storage capacity of the slurry. Slurry flow with presence of phase change particles was examined by Roy and Avanic [6]. They showed that Stefan number was the key parameter to determine the amount of heat flow towards the system. Chen et al. [7] studied a laminar flow and heat transfer in a flow system with existence of micro-sized particles. The findings revealed that thermal performance lowered notably because of the pump power due to high viscosity of the slurry. Thermal analysis of micro-encapsulated

slurries in a horizontal circular tube was carried out by Wang et al. [8]. They introduced a new correlation estimating the heat transfer rates for improved design configuration of the thermal flow system.

Although thermal performance of the volumetric solar absorbers are investigated previously [9-11], the study needs to be extended due to complex nature of the thermal storage system. Therefore, in the present study thermal performance characteristics of volumetric solar absorption system including absorber plate and slurry flow in a channel with presence of phase change particles are examined. The effect of absorber plate on the thermal performance of the system is examined for two solar concentrations. Thermal performance and pump power loss parameters are introduced to estimate the thermal response of the volumetric solar absorbing system to the various solar concentrations. Water is used as a carrier fluid and Lauric acid is incorporated as phase change particles in the flow system. Since the assessment of the performance of the solar heater is based on the solar concentration, the average radiation from the sun is incorporated in the analysis rather than time variation along the day, months, and year. Consequently, the simulation results provide insight into the average values of solar irradiation at different concentrations. Numerical study is extended to simulate the previous study [1] for the model validation purposes.

HEATING ANALYSIS

The working fluid is assumed to be homogenous in the analysis due to low volumetric concentration of the phase change particles, which is 5% in the carrier fluid. A laminar slurry flow in a rectangular channel with the presence of absorbing plate is considered in the analysis. Water is used as a carrier fluid and Lauric acid is incorporated as PCM. The top surface of the channel is exposed to a solar radiation at two different concentrations. A schematic view of the flow situation, resembling the channel and the absorber plate in the channel, is shown in figure (1). The governing conservation equations are:

Continuity equation:
$$\nabla \cdot \vec{v} = 0 \qquad (1)$$

Momentum equation:
$$\nabla \cdot \left(\rho_{eff} \vec{v}\vec{v} \right) = -\nabla p + \mu_{eff} \nabla^2 v + \vec{F} \qquad (2)$$

Energy equation:
$$\nabla \cdot \left(\vec{v} \left(\rho_{eff} E + p \right) \right) = \nabla \cdot \left(k_{eff} \nabla T \right) + S \qquad (3)$$

where v is the flow velocity, p is the pressure, E is the energy, ρ_{eff} is the effective density, k_{eff} is the effective thermal conductivity, S is the source term due to radiation absorption. The effective properties of the working fluid are defined according to the equations reported in the open literature [12-15]. Although the geometric shape and the size of the PCM

(phase change particles) slightly influence the effective properties [12], the data used for the standard PCM are incorporated in the calculations [15]. The density of the effective fluid is calculated using mass balance as [11]:

$$\rho_{eff} = c\rho_p + \left(1-c\right)\rho_f \qquad (4)$$

where ρ_p is the density of the phase change particles, ρ_f is the carrier fluid density, and c is the concentration.

The effective thermal conductivity using Maxwell's model [14] is:

$$k_{eff} = k_f \frac{2 + {k_p}\big/{k_f} + 2c\left({k_p}\big/{k_f} - 1 \right)}{2 + {k_p}\big/{k_f} - c\left({k_p}\big/{k_f} - 1 \right)} \qquad (5)$$

where k_f is the fluid thermal conductivity and k_p is the PCM thermal conductivity.

The effective bulk viscosity calculation of is based on Vand's correlation, which is [15]:

$$\mu_{eff} = \left(1 - c - 1.16c^2\right)^{-2.5} \mu_f \qquad (6)$$

where μ_f is the fluid viscosity and c is the concentration.

The effective specific heat of the working fluid is calculated using the energy balance, which is [12]:

For $T_p < T_{solidus}$:

$$c_{p_{eff}} = \frac{c\left(\rho c_{p,S} \right)_p + \left(1-c\right)\left(\rho c_p \right)_f}{\rho_b} \qquad (7)$$

for $T_{solidus} < T_p < T_{liquidus}$:

$$c_{p_{eff}} = \frac{c\left(\rho\left(\frac{c_{p,S}+c_{p,L}}{2} + \frac{L_{fusion}}{T_{liquidus}-T_{solidus}}\right)\right)_p + (1-c)(\rho c_p)_f}{\rho_b}$$

(8)

for $T_P > T_{liquidus}$:

$$c_{p_{eff}} = \frac{c(\rho c_{p,L})_p + (1-c)(\rho c_p)_f}{\rho_b}$$

(9)

where $(c_p)_f$ is the specific heat of the carrier fluid, $(c_{p,S})_p$ is the specific heat of the PCM particle in solid state and $(c_{p,L})_p$ is the specific heat of the PCM particle in the liquid state, T_p is the PCM temperature, $T_{liquidus}$ is liquid temperature at phase change, and $T_{solidus}$ is the solid temperature at phase change.

The governing equation for the radiative transport related to volumetric absorption system is:

$$\nabla \cdot (I(\vec{r},\vec{s})\vec{s}) + a.I(\vec{r},\vec{s}) = an^2 \frac{\sigma T^4}{\pi}$$

(10)

where I is the radiation intensity, a is the absorption coefficient, n is the refractive index, and T is the local temperature. The absorbing plate is placed at different locations in the channel (figure (1)). However, for different locations of the absorbing plate, the channel height is considered to be 5 mm, the total channel length is kept as 1.5m and the remaining sections of the channel are opaque. The absorbing plate consists of a selective surface, which is coated at the top of the silver plate of 0.5 mm thickness. In this case, Zr-N coating is considered on the silver plate, with the coating thickness of 0.16 μm. It should be noted that use of Zr-N improves significantly the absorption of solar radiation by the plate [25]. In the analysis, three cases are incorporated. In the first case, the absorbing plate (coated plate) is placed at the top surface of the channel and Zr-N coating is exposed to the solar radiation; therefore, the solar absorption takes place in the top coating. In the second case, the absorbing plate is located at the bottom of the channel with a glass cover at the top surface of the channel. The glass cover provides the structural integrity at the channel surface and transmits the solar radiation into the channel. In this case, the transmitted radiation is volumetrically absorbed in the fluid and remaining radiation is absorbed by the absorbing plate at the channel bottom. In the third case, a semi-transparent absorbing plate is added to case 2 in such a way that majority of the incident radiation is absorbed at the middle height of the channel where a semi-transparent

absorbing plate is located. The absorbing plate at bottom of the channel enables the absorption of the radiation transmitted from the semi-transparent absorbing plate. This arrangement provides the total absorption of the incident radiation in the channel.

The surface of the absorbing plate has high absorption and low emittance, thus has the ability to harness the solar energy effectively while limiting the losses due to emission. Zirconium Nitride coating on Silver (ZrN –Ag) tends to follow good pattern for selective surface having transition wavelength centered a 2 μm [15]. It has absorptance of 0.86 and emittance of 0.039 at 600 K, with conversion efficiency of 0.52 [16]. The conversion efficiency can be used to determine the usefulness of solar selective surface, which is [17]:

(9)

$$CE = \frac{Q_a - Q_e}{Q_s}$$

(11)

where Q_a is the absorbed solar flux, Q_e is the emitted solar flux and Q_s is the incoming solar flux.

Boundary Conditions:

Flow Inlet: The laminar flow in the channel is assummed. A uniform velocity boundary condition at inlet is selected and inlet temperature is set at T_{in} = 298K, which is fixed for all the cases simulated. The fluid velocity is varied in each case within the range of Reynolds numbers of 50, 100, 200 and 500.

Flow outlet: Pressure Outlet Boundary Condition is used representing discharge of the flow into open atmosphere (gauge pressure = 0).

Solid Wall: No-slip condition is assumed at the solid wall, such that the velocity at the solid wall is 0.

Irradiated wall: Discrete Ordinate Method (DOM) is used to define the solar radiation on the irradiated channel surface (figure (1)). The top surface of channel is also assumed to be in contact with atmosphere resulting in radiation and convection losses to surrounding, which can be written as:

$$q = h_{ext}(T_{ext} - T_w) + \varepsilon_{ext} \, \sigma \, (T_\infty^4 - T_w^4)$$ (12)

Non-conformal Interface: Non-conformal meshing is used to model the absorbing surface. A mesh interface is defined for coupling the two surfaces. The interface is between two solid regions; such interface is thermally coupled.

Outer walls: The bounded walls for the setup are all assumed to be opaque and adiabatic, except for the irradiated wall (top surface of the channel (figure (1)). In the case of opaque treatment, no radiation is transferred through the surface. The Adiabatic wall treatment assumes no heat transfer from the surface to its outer surroundings while representing insulated boundary.

Radiation boundary condition at the channel walls: Opaque wall boundary condition is assumed at the channel wall,

except at the top surface of the channel. Opaque wall boundary takes into consideration the emission from the wall with part of the incoming radiation on the wall being absorbed and the remaining radiation reflected back into the fluid. The boundary treatment for semi transparent wall at the top surface is incorporated. The interface reflectivity at semi-transparent wall is based on the Fresnel Equation. The reflection from the solid surfaces is considered to depend on the refractive index.

In order to assess the influence of absorbing plate on the thermal performance of the channel, the performance parameters are introduced in line with the previous study [9-11]. These include the performance parameter (the heat gain by the flow over the heat input by the solar radiation in the channel, Q_{gain}/Q_{in}), and pump power lost parameter (pump power loss over the heat gain by the fluid in the channel, ($\dfrac{h_{p,L}}{Q_{gain}}$).

Therefore, the performance parameters are:

$$E = Q_{gain} / Q_{in}$$
(13)

and

$$h_L = h_{P,L} / Q_{gain}$$
(14)

where

$$Q_{in} = C \times I \times A \quad ; \quad Q_{gain} = \dot{m} \cdot C_p \cdot \left(T_{out} - T_{in}\right) \quad \text{and}$$

$$h_{P,L} = \dot{V} \cdot \Delta P \quad \text{where} \quad \dot{V} = \dot{m} / \rho \; .$$

The heat transfer coefficient is calculated as:

$$h = \frac{q''}{T_w - T_b}$$
(15)

where q'' is the heat flux, and T_w and T_b are the wall and fluid bulk temperatures, respectively. The Nusselt Number can be calculated as:

$$Nu = \frac{hD_h}{k}$$
(16)

NUMERICAL SOLUTION

Fluent CFD code [26] is used in the simulations. The control volume approach is incorporated to discretize the governing equations. The SIMPLE scheme is used for pressure-velocity coupling and the nonlinear set of equations is solved using iterative method with satisfying the convergence criterion. In this case, the residuals are set to 10^{-6} for continuity and momentum, and 10^{-10} for energy. In addition, surface monitors

at the outlet are monitored for velocity and temperature to ensure convergence.

Equation 10 is used to determine the radiation intensity in the spatial Cartesian system (x,y,z). The radiation equation is, then iteratively solved, for each of the solid angles. The uncoupled implementation of Discrete Ordinate Method (DOM) is used to solve radiation equation. It should be noted that this method is suitable for the solution of radiation problems associated with the low optical thicknesses. The equations for the energy (Eq.3) and radiation intensities (Eq.10) are solved one by one, assuming prevailing values for other variables [18]. In DOM, the radiative transfer equation (RTE) is solved for finite number of discrete solid angles, which are determined by the angular discretization. Each solid angle is associated with a vector direction $\vec{s}$, which is fixed in relation to the Global Cartesian System (x,y,z).
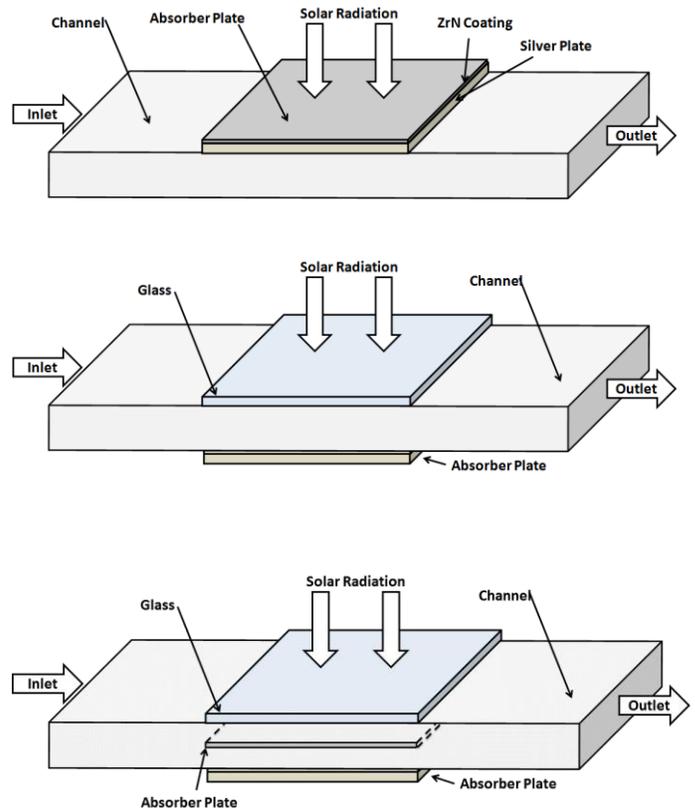
Figure 1. A schematic view of volumetric absorption system.

RESULTS AND DISCUSSION

The performance characteristics of solar volumetric absorption system consisting of absorber plate and channel flow with presence of phase change particles are investigated for two solar concentrations. The absorber plate is placed in three different locations in the channel to assess the influence of

absorber plate location on the heat transfer rates in the channel. The absorber plate consists of a selective surface, which is ZrN coating onto a silver plate.

In order to validate the model used in the simulations, the dimensionless temperature values are reproduced in line with the geometric configurations and the respective boundary conditions presented in the previous study [1]. The identical conditions and geometry provide the comparison of dimensionless temperature data obtained from the analytical solution [1] and the model predictions. It is found that dimensionless temperatures predicted from the present simulations and those obtained from the previous work [1] are in good agreement.

Figures (2) and (3) show the Nusselt number variation along the absorber plate for different solar concentrations. It should be noted that the absorber plate location is at the top surface of the channel (figure (1)). The Nusselt number reduces along the length of the absorber plate and this reduction increases at high solar concentrations. Since the concentration of the phase change particle is 5%, phase change particles melts almost instantly in the carrier fluid because of the attainment of high temperature in the vicinity of the absorber plate surface. In this case, introducing high solar concentration at the absorber surface enhances temperature of absorber plate and fluid temperature in the vicinity of the absorber plate surface. This, in turn, lowers temperature difference between absorber and working fluid; hence, reducing the Nusselt number along the absorber plate surface. As the solar concentration reduces (C = 5), difference between the absorber plate wall temperature and temperature of working fluid in the absorber plate vicinity remains small, which leads to some small changes in the Nusselt number. The Nusselt number reduces slightly in the close region of the absorber plate, which occurs for solar concentration C = 5. This behavior is attributed to the end of phase change of process (completion of the melting of PCM) where fluid temperature increases to the liquidus temperature. Hence, the fluid temperature increases due to sensible heating in the flow system while lowering temperature difference between the absorber plate wall and its neighborhood fluid. As a consequence of this behavior, the Nusselt number attains slightly low values in this region.

Figures (4) and (5) show the performance parameter (Q_{gain}/Q_{in}) with the Reynolds number at different locations of absorber plate for different solar concentrations. The solar concentration has a significant effect on the performance parameter; however, the location of absorber plate alters this effect. In this case, operating solar volumetric absorber system incorporating the absorber plate at the mid-height of the channel lowers the thermal performance of the system. The comparison of the absorber plate in the channel reveals that the absorber plate at the top of the channel results in the highest performance parameter. Consequently, using the selective surface with low reflectivity and emissivity at the top of the channel gives rise to the highest performance parameter for the range of solar concentrations and volume fractions of phase change particles

used in the system. In addition, operating the system at high solar concentration improves the performance parameter notably.
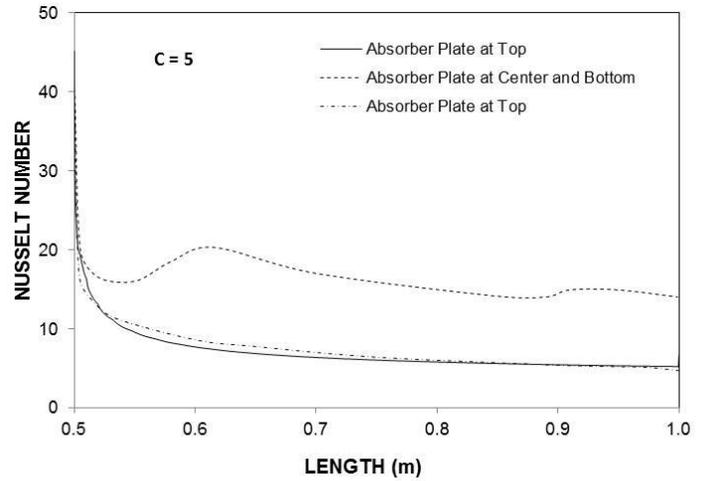
Figure 2. Nusselt number variation along the absorber plate surface for solar concentration C = 5.
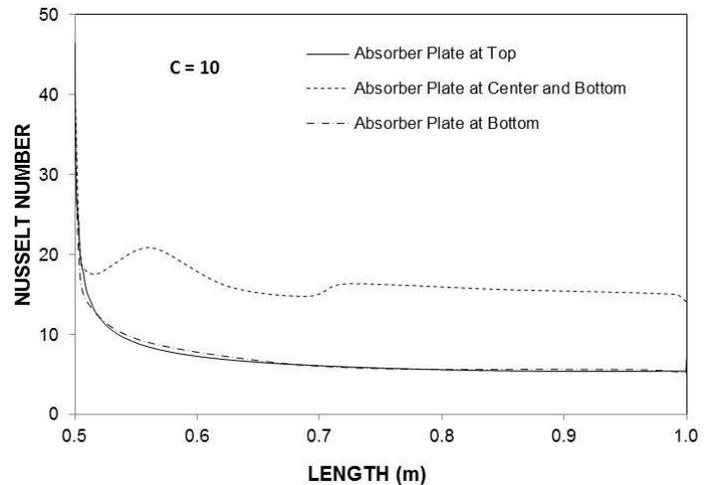
Figure 3. Nusselt number variation along the absorber plate surface for solar concentration C = 10.

Figure (6) shows pump power loss parameter, as at different locations of the absorber plate in the channel. The pump power loss is closely related to the fluid frictional loss in the channel because of the presence of the absorber plate at the mid-height of the channel. The pump power loss parameter increases at high Reynolds number. Since the fluid friction increases with increasing rate of fluid strain at high Reynolds number, the pump power loss parameter also rises at high Reynolds numbers. The absorber plate surface is at the same elevation of the channel wall when its locations are at the top and the bottom surfaces of the channel. Therefore, the pump

power loss parameter becomes identical at these locations of the absorber plate. The pump power loss parameter attains large values for the case where the absorber plate is located at the mid-height of the channel. This is due to the fact the enhancement of the frictional loss because of the exposure of the absorber plate surfaces to the working fluid.
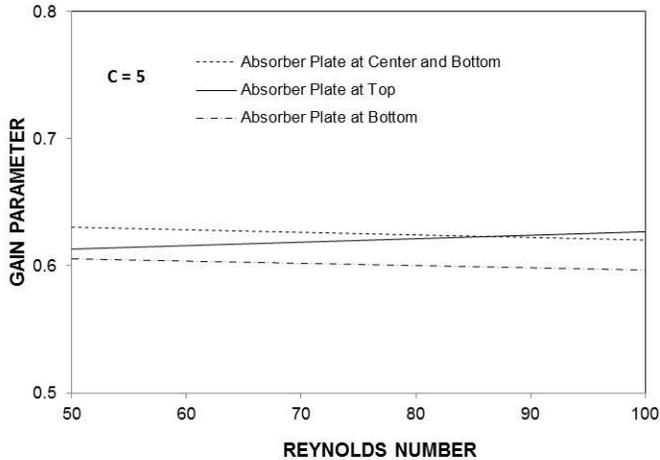
Figure 4. Thermal gain parameter with Reynolds number for solar concentration C = 5.
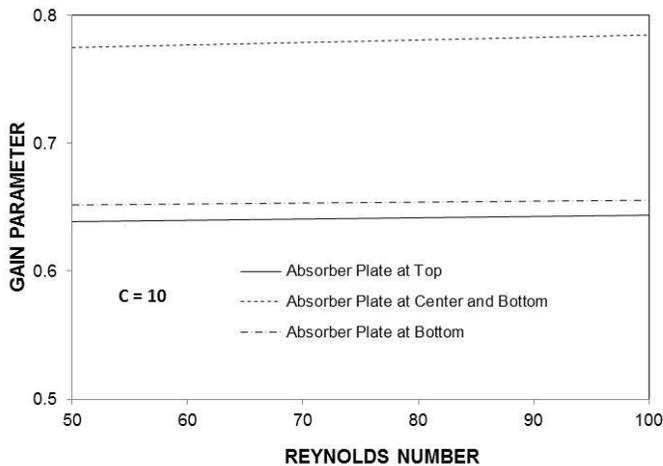
Figure 5. Thermal gain parameter with Reynolds number for solar concentration C = 10.

CONCLUSION

Thermal performance of a volumetric solar absorber, consisting of an absorber plate and phase change material in a channel, is simulated for various solar concentrations. Lauric acid as a phase change particles with 5% volume concentration is used in the carrier fluid. The absorber plate location is varied in the channel and the location of absorber plate on the thermal performance of the solar absorber is evaluated. A ZrN thin coating (16 μm) are placed on a silver plate to resemble the absorber plate. The findings revealed that the Nusselt number along the absorber plate surface increases for the case where the

absorber plate is located at the mid-height of the channel. The phase change process in the neighborhood of the absorber plate surface is responsible for the Nusselt number increase along the plate surface. From the simulation data, the considerable amount of absorbed solar intensity takes place by the absorbing plate in the channel. The performance parameter is influenced by the concentration of the phase change material and the Reynolds number; in which case, increasing Reynolds number enhances the performance parameter, which becomes substantial with increasing concentration. The performance parameter reduces for the case of the absorber plate located at the mid-height and at the bottom of the channel. However, it attains the highest when the absorber plate is located at the top surface of the channel. Hence, the volumetric solar absorption system operating at high Reynolds number with the absorber plate location at the top of the channel resulted in high performance parameters. The pump power loss parameter attains high values for the case of the absorber plate located at the mid-height of the channel.
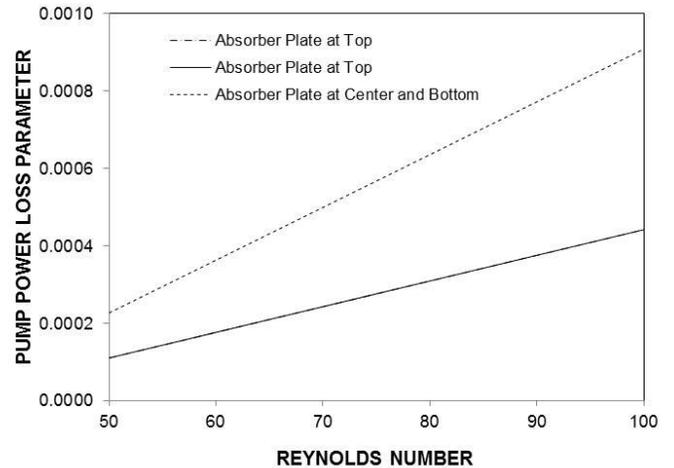
Figure 6. Pump power loss parameter with Reynolds number.

REFERENCES
1. A. Veeraragavan, A. Lenert, B.S. Yilbas, S. Al-Dini, E. Wang, Analytical model for the design of volumetric solar flow receivers. Int. J. of Heat and Mass Transfer, Vol. 55, n 4, pp. 556-564, 2012.
2. P. Charunyakorn, S. Sengupta, and S.K. Roy, Forced convection heat transfer in microencapsulated phase change material slurries : flow in circular ducts, Int. J. Heat Mass Transfer, Vol. 34(3), pp. 819-833, 1991.

3. S.K. Roy, and S. Sengupta, An evaluation of phase change microcapsules for use in enhanced heat transfer fluids, International communications in heat and mass transfer, 18(4), pp. 495-507, 1991.

4. E. Choi, Y.I. Cho, and H.G. Lorsch, Forced convection heat transfer with phase-change-material slurries:turbulent flow in a circular tube, Int J. Heat Mass Transfer, 37(2), pp. 207-215, 1994.

5. M. Goel, S.K. Roy and S. Sengupta, Laminar forced convection heat transfer in microcapsulated phase change material suspensions, Int. J. of Heat and Mass Transfer, Vol. 37(4), pp. 593-604, 1994.

6. S.K> Roy, and B.L. Avanic, Laminar Forced Convection Heat Transfer With Phase Change Material Emulsions, Int. Comm. Heat Mass Transfer, 24(5), pp. 653-662, 1997,.

7. B. Chen, X. Wang and Y. Zhang, Experimental research on laminar flow performance of phase change emulsion, Applied Thermal Engineering, 26, pp. 1238-1245, 2006.

8. X. Wang,J. Niu, Y. Li, X. Wang, B. Chen, R. Zeng., Q. Song and Y. Zhang, Flow and heat transfer behaviors of phase change material slurries in a horizontal circular tube, Int. J. of heat and mass transfer, 50(13-14), pp. 2480-2491, 2007.

9. O.S. Kaleem and B.S. Yilbas, Thermal characteristics of volumetric solar absorption system incorporating absorber plate in the channel flow, Int. J. of Energy Research, DOI: 10.1002/er.3063, 2013.

10. O.K. Siddiqui and B.S. Yilbas, Solar absorption heating in horizontal channel: influence of absorbing plate location on thermal performance, Energy Conversion and Management Vol. 74 , pp. 140-148, 2013.

11. O.K. Siddiqui and B.S. Yilbas, Performance characteristics of volumetric solar receiver: presence of absorber plate with a selective surface, Numerical Heat Transfer, Part A., in press, 2014.

12. A.B.S. AlQuaity, S.A. Al-Dini, B.S. Yilbas, Investigation into Thermal Performance of Nanosized Phase Change Material (P.C.M.) in Microchannel Flow, Int. J. of Numerical Methods for Heat and Fluid Flow, v 23, n 2, p 233-247, 2013.

13. R. Sabbah, M.M. Farid, and S. Al-Hallaj, Micro-channel heat sink with slurry of water with micro-encapsulated phase change material:3D-numerical study, Applied Thermal Engineering, Vol. 29, pp. 445-454, 2008.

14. J.C. Maxwell, A Treatise on Electricity and Magnetism, Vol. 1, Dover Publications, New York, 1954.

15. X. Wang, J. Niu, Y. Li, X. Wang, B. Chen, R. Zeng, Song Q., and Zhang Y., Flow and heat transfer behaviors of phase change material slurries in a horizontal circular tube, International journal of heat and mass transfer, 50(13-14), pp. 2480-2491, 2007.

16. R. Blickensderfer, Solar Absorbers—Selective Surfaces, in: Electric Refractory Materials, 2000

17. F. Mammadov, Study of Selective Surface of Solar Heat Receiver, Int. J. of Energy Engineering, Vol. 2, pp. 138-144, 2012.

18. Product Documentation, Fluent 12.1., ANSYS Inc., 2011.